

# Journal Pre-proof

Effect of TiO<sub>2</sub> and Gadolinium dopants on photocatalytic behavior for Acriflavine dye

UmarFarooq R. Bagwan, Irfan N. Shaikh, Ramesh S. Malladi, Abdulazizkhan L. Harihar, Shirajahammad M. Hunagund



PII: S1002-0721(19)30129-2

DOI: <https://doi.org/10.1016/j.jre.2019.09.006>

Reference: JRE 598

To appear in: *Journal of Rare Earths*

Received Date: 14 February 2019

Revised Date: 22 August 2019

Accepted Date: 12 September 2019

Please cite this article as: Bagwan UR, Shaikh IN, Malladi RS, Harihar AL, Hunagund SM, Effect of TiO<sub>2</sub> and Gadolinium dopants on photocatalytic behavior for Acriflavine dye, *Journal of Rare Earths*, <https://doi.org/10.1016/j.jre.2019.09.006>.

This is a PDF file of an article that has undergone enhancements after acceptance, such as the addition of a cover page and metadata, and formatting for readability, but it is not yet the definitive version of record. This version will undergo additional copyediting, typesetting and review before it is published in its final form, but we are providing this version to give early visibility of the article. Please note that, during the production process, errors may be discovered which could affect the content, and all legal disclaimers that apply to the journal pertain.

© [Copyright year] Published by Elsevier B.V. on behalf of Chinese Society of Rare Earths.

# Effect of TiO<sub>2</sub> and Gadolinium dopants on photocatalytic behavior for Acriflavine dye

UmarFarooq R. Bagwan<sup>1</sup>, Irfan N. Shaikh<sup>1</sup>, Ramesh S. Malladi<sup>2</sup>, Abdulazizkhan L.

Harihar<sup>3</sup> and Shirajahammad M. Hunagund<sup>4\*</sup>

<sup>1</sup> Department of Chemistry, SECAB Institute of Engineering and Technology, Vijayapur-586101, Karnataka, India

<sup>2</sup> Department of Chemistry, BLDEA's V.P.Dr. P.G. Halakatti college of Engineering and Technology, Vijayapur-586103, Karnataka, India

<sup>3</sup> Department of Chemistry, Kittel Science College, Dharwad-580001, Karnataka, India

<sup>4</sup> Center for Nanoscience and Nanotechnology, SECAB Institute of Engineering and Technology, Vijayapur-586101, Karnataka, India

\*Corresponding author email: [shiraj.034@gmail.com](mailto:shiraj.034@gmail.com)

## Abstract:

Herein, we report the experimental methodology to optimize the operational parameters of the photocatalytic degradation of acriflavine dye using TiO<sub>2</sub> and Gd<sup>+3</sup> as dopant. A series of Gd<sup>+3</sup> doped TiO<sub>2</sub> nanoparticles were synthesized via hydrothermal route and characterized using various techniques like FT-IR, UV, XRD, FESEM and EDS. It was observed that synthesized particles were in the range of 25 to 30 nm with spherical shape in nature. TiO<sub>2</sub> has rutile phase and the average particle size was estimated from Scherrer's equation. Energy bandgap was estimated using Tauc's plot. The photodegradation was carried out under UV light in pseudofirst order condition. To understand the kinetics, four experimental parameters were chosen as independent variables like percentage of dopant, initial concentration of dye, dosage of catalyst and pH of reaction medium. The degradation efficiency of 92 % was observed for 0.5% Gd doped TiO<sub>2</sub> at catalyst dosage of 0.3g dm<sup>-3</sup>, pH 10 and dye concentration of 3 x10<sup>-6</sup> mol dm<sup>-3</sup>. It was observed that, the photocatalytic activity of TiO<sub>2</sub> can be increased by using Gadolinium as dopant only in optimum concentration. Further, this photocatalyst can be employed to degrade other organic pollutants.

**Keywords:** TiO<sub>2</sub>, Gadolinium, Acriflavine, Hydrothermal, Photocatalytic activity, Kinetics

---

\* **Foundation item:** This research did not receive any specific grant from funding agencies in the public, commercial, or not-for-profit sectors.

\* Corresponding author: Center for Nanoscience and Nanotechnology, SECAB Institute of Engineering and Technology, Vijayapur-586101, Karnataka, India  
Email: [shiraj.034@gmail.com](mailto:shiraj.034@gmail.com) Mob:+919164343266

## 1. Introduction

Water is the most essential component for the existence of life on earth. Water resources are continuously being exploited due to rapid industrialization from mid of the last century. Many organic pollutants persist in water and have been detected in the range from ng/l to mg/l<sup>1</sup>, but it has made adverse effect on environment. Sensitive receptors such as phytoplankton, zooplankton, including human beings and animals are facing life threatening problems<sup>2</sup> over the last decade due to gradual change in aquatic environment and interaction with food chain. Water resources are polluted due to organic contaminants which are discharged by manufacturing industries, pharma industries, fertilizer industries, chemical industries, textile and dyeing industries<sup>3</sup>. Further, the municipal waste-water, runoff from agricultural procedures and chemical spills also contribute towards contamination of water resources. Organic contaminants persist in water and enter in biological food chain which affects human health and entire ecosystem. In recent years, environmentalists and scientists have raised serious concern over growing deterioration in quality of water. Today's challenge is to get clean water which should be free from color, odor, contaminants and pollutants.

Acriflavine [AFN] is used as an antiseptic since the World War. It was synthesized in 1912 by a German medical researcher, Dr. Paul Ehrlich<sup>4</sup>. Acriflavine hydrochloride is soluble in water and generally employed to treat fungal infections of aquarium fish. It is also used in biochemistry due its fluorescent property. Despite its medicinal importance, acriflavine is also known for its harmful effects on human beings such as skin irritation, eye irritation, breathing problems<sup>5</sup>. Acriflavine is also found to be toxic to aquatic plants. It also imparts fluorescent color to water which is required to be removed to meet the ideal characteristics of clean water.

In recent years, TiO<sub>2</sub> has emerged as a promising heterogeneous catalyst among numerous semiconductors and attracted researchers for having versatile properties like chemical stability, non-toxicity towards environment and cost effectiveness<sup>6</sup>. The holes and electrons generated upon photoexcitation have better oxidizing and reducing properties respectively. It has band gap between 3.0 eV to 3.2 eV<sup>6</sup> which requires UV light within 415 nm for excitation. Several attempts have been made to enhance photocatalytic activity<sup>7,8</sup> via doping with inner transitional elements like La<sup>+3</sup>, Eu<sup>+3</sup>, Nd<sup>+3</sup>, Gd<sup>+3</sup>, Pr<sup>+3</sup><sup>9</sup>. The lanthanides are preferred to enhance the photocatalytic activity<sup>10</sup> of TiO<sub>2</sub> because they have vacant f-orbitals<sup>11</sup> which are capable to make complex efficiently with functional groups of organic compounds such as aldehydes, ketones, alcohols, amines, thiols etc<sup>12</sup>. The complex forming ability of lanthanides make dye molecules to adsorb on TiO<sub>2</sub> surface to larger extent which facilitates photodegradation<sup>12</sup>. Higher the adsorption dye molecules on the surface of TiO<sub>2</sub> matrix, higher would be the efficiency of photodegradation<sup>13</sup>. Intrigued by the above observations, herein, we report the low cost heterogeneous photocatalyst, Gd doped TiO<sub>2</sub> for

degradation of acriflavine<sup>14</sup>. Further, we have studied the effect of various parameters such as dye concentration, doses of photocatalyst and pH of solution on the rate of photodegradation.

## 2. Details of Experiment and methods used.

### 2.1 Chemicals and reagents.

Titanium (IV) butoxide [ $\text{Ti}(\text{OBU})_4$  or  $\text{Ti}(\text{OC}_4\text{H}_9)_4$ ] was purchased from Alfa Aesar chemicals, India. Nitric acid was purchased from Nice chemicals, India. Acriflavine hydrochloride and Gadolinium(III) Nitrate were purchased from Sigma Aldrich. The pH of solution was maintained using buffer solutions, analytical grade chemicals were used to maintain required pH. Acetate and phosphate buffer were used to maintain acidic medium (pH 4.0 to 5.0) and neutral medium (6.5 to 8.5) respectively. Basic medium (pH 9.0 to 10.0)<sup>15</sup> was maintained using borate buffer solution. All solutions used in experiments were prepared using milli pore water.

#### 2.1.1 Instruments employed for Experiments and Characterization.

1. **Kinetic study:** The degradation kinetics was followed using Analytika Jena Specord 200 plus UV- Visible spectrophotometer.

2. **Degradation study:** A mercury lamp (Philips, TUV 10W,  $E_{\text{max}} = 254 \text{ nm}$ ) mounted in lab made cabinet was used for degradation study. The light intensity falling on reaction mixture was  $5 \text{ mWcm}^{-2}$

3. **Band gap measurement:** The Analytika Jena, Specord 200 plus UV- Visible spectrophotometer with Win Aspect Software was used for absorption and band gap measurements.

4. **Functional group identification:** A FT-IR spectrophotometer (Nicolet 6700, USIC, Karnataka University Dhrawad) was used for functional group confirmation. The sample was analyzed between  $4000 \text{ cm}^{-1}$  to  $400 \text{ cm}^{-1}$  in KBr pellet at resolution of  $2 \text{ cm}^{-1}$ .

5. **Detection of Crystal structure and particle size:** A X-ray Diffractometer (XRD, Cu Source,  $\lambda = 0.15 \text{ nm}$ , Rigaku pro analytical, Manipal Institute of Technology, Manipal) was used to detect crystal structure and particle size. The samples were analyzed by scanning at the rate of  $0.02^\circ$  per second in the range between  $20^\circ$  to  $80^\circ$ .

6. **Surface Morphology and Elemental Composition:** Field Emission Scanning Electron Microscope (FESEM) was used to study the surface morphology. The elemental composition was ascertained by Energy dispersive detector (EDS), DST-PURSE Laboratory, Mangalore University, Manglore.

7. **pH measurement:** The pH of solution was measured using Systronics pH meter.

### 2.2 Hydrothermal synthesis of $\text{TiO}_2$ and $\text{Gd-TiO}_2$

Titanium(IV) butoxide was used as precursor for the synthesis of  $\text{TiO}_2$  nanoparticles by hydrothermal method. A mixture of 15 ml water and 15 ml concentrated Nitric acid were taken in 100 ml beaker. 0.6 ml of titanium(IV) butoxide solution was added dropwise with constant stirring and the mixture was stirred for 1 h. The clear solution was transferred into a

Teflon lined stainless steel autoclave, the auto-clave was tightly sealed and placed in hot air oven at 180<sup>0</sup> C for 3 h<sup>16</sup>. Then, the auto-clave was cooled to ambient temperature. The reaction mixture was centrifuged to obtain a fine powder. The product was washed repeatedly with milli-pore water and ethanol. Later it was dried in hot air oven at 100<sup>0</sup> C for 1 h.

The TiO<sub>2</sub> was doped using Gd for which Gadolinium nitrate was used in mole ratio of 0.2%, 0.3 %, 0.5% and 1.0% to TiO<sub>2</sub>. The dopant was dissolved in mixture of 15 ml water and 15 ml concentrated HNO<sub>3</sub> and rest of the procedure is same as mentioned above.

### 2.3 Photodegradation study

In order to study the photocatalytic degradation of acriflavine, a known concentration of acriflavine solution was taken in 100 ml beaker. The pH of solution was maintained using buffer solution and 0.3g dm<sup>-3</sup> of TiO<sub>2</sub> nanoparticles was added as photocatalyst. The solution was kept in dark for 2 h to achieve adsorption equilibrium between substrate and photocatalyst. After that, the beaker was placed under 10 W UV-lamp (Philips) mounted in lab-made UV irradiation cabinet. During the illumination, the solution was stirred continuously with the help of magnetic stirrer. The decrease in concentration of acriflavine was monitored by measuring the decrease in absorbance at 262 nm using UV-visible spectrophotometer. For every 15 min, the analyte was taken out for the measurement of absorbance at 262 nm. Before the measurement, the solution was centrifuged for 10 min at 5000 rpm to remove any turbidity. All kinetic data were evaluated using Microsoft Excel 2010 program.

## 3. Results and Discussions

### 3.1 Characterization of TiO<sub>2</sub> and Gd-TiO<sub>2</sub>

Samples were subjected to X-ray diffraction studies to ascertain the crystal structure and particle size. The XRD patterns were obtained by using Cu source at wavelength of 0.15 nm and scanning at the rate of 0.02<sup>0</sup> per second in the range between 20<sup>0</sup> to 80<sup>0</sup>.

The XRD pattern for pure TiO<sub>2</sub> is shown in **Fig. 1a**, the observed Bragg reflection peaks at 2θ and corresponding reflection planes are 27.392° (110), 35.087° (101), 39.126° (200), 41.230° (111), 43.970° (210), 54.275° (211), 56.528° (220), 62.823° (002), 68.921° (301), 69.841° (112) and 82.217° (321). The 2θ values obtained in XRD pattern were compared with data sheet no 89-0552 of Standard Joint Committee on Powder Diffraction Standards (JCPDS). It exhibits that the pure TiO<sub>2</sub> is having rutile phase with tetragonal structure. The XRD pattern of pure TiO<sub>2</sub> shows sharp, broad and strong peaks which indicates TiO<sub>2</sub> formed is crystalline in nature.

The **Fig. 1b** represents XRD pattern for Gd doped TiO<sub>2</sub>, the observed Bragg's reflection peaks at 2θ and corresponding reflection planes are 27.331°(110), 35.833° (101), 39.037° (200), 40.982° (111), 43.870° (210), 54.023° (211), 56.395° (220), 62.213° (002), 63.779° (310), 68.642° (301), 69.234°(112), 81.898° (321) and 83.861° (400). The 2θ values obtained in XRD pattern were compared with data no 89-6975 of JCPDS which confirms Gd doped TiO<sub>2</sub> is having Rutile phase and tetragonal structure. The average particle size is calculated using Scherrer's equation<sup>17</sup>. The estimated values for TiO<sub>2</sub> and Gd doped TiO<sub>2</sub> are 20.89 nm and 13.12 nm respectively. The width of diffraction peak increases after doping with Gadolinium<sup>18</sup>, which may be due to decrease in grain size. According to Scherrer's

equation, the width of diffraction peaks are inversely proportional to crystal size. Hence after doping, the particle size reduces due to which increase in width of diffraction peak is observed<sup>19</sup>. Further, it is not anticipated Gd<sup>+3</sup> to enter in crystal lattice of TiO<sub>2</sub>, because the ionic radius of Gd<sup>+3</sup> (0.94 Å) is greater than the Ti<sup>+4</sup> (0.68 Å)<sup>20</sup>. Hence Gd<sup>+3</sup> ions, rather deposit on the surface and grain boundaries of TiO<sub>2</sub> matrix. The intensity of diffraction peaks increases with increase in concentration of dopant atoms. Generally, the peak intensities are being affected by electron density, when dopant concentration increase the electron density increases due to large size of Gd<sup>+3</sup> ions. Thus, doping with more number Gd<sup>+3</sup> ions incorporates more number of scattering centers which enhances the peak intensity.<sup>20</sup>

FESEM was employed to study the surface morphology of pure TiO<sub>2</sub> and Gd doped TiO<sub>2</sub>. The FESEM images of pure TiO<sub>2</sub> and Gd-doped TiO<sub>2</sub> are shown in **Fig. 2(a,b)** and **Fig. 2(c,d)** respectively which reveals the average particle size of pure TiO<sub>2</sub> is about 30nm, whereas average particle size of Gd doped TiO<sub>2</sub> nanoparticles are of 25nm. Particles of both pure and Gd doped TiO<sub>2</sub> are in spherical in shape. The decrease in particle size is observed with doping, perhaps due to restriction in crystal growth imposed by Gd<sup>+3</sup> owing to its adsorption on active sites of TiO<sub>2</sub> matrix<sup>12</sup>. The EDX spectrum of pure TiO<sub>2</sub> represents the peaks corresponding to Ti and O. Similarly, the EDX spectrum of Gd doped TiO<sub>2</sub> represents presence of Gd, Ti, and O. Trace amount of residual carbon is also found in both the samples. (Available as supplementary data)

The UV-visible spectral analysis was carried from 300 nm to 600 nm. The UV-visible spectra of both pure TiO<sub>2</sub> and Gd doped TiO<sub>2</sub> is shown in **Fig 3** which reveals that pure TiO<sub>2</sub> shows maximum absorption at 344nm and gadolinium doped TiO<sub>2</sub> shows the maximum absorption at 317nm. The absorption maximum is shifted to lower wavelength which indicates the presence of Gadolinium in TiO<sub>2</sub> matrix. For the estimation of band gap of TiO<sub>2</sub> and Gd-TiO<sub>2</sub> Tauc's plot were plotted and it is shown in the **Fig. 4** The estimate band gap for TiO<sub>2</sub> and Gd-TiO<sub>2</sub> is 3.06 eV and 3.54 eV respectively<sup>17</sup>. As the particle size decreases, the grain size decreases and less number of atomic orbitals overlap and discrete electronic bands are formed, due to which the band width reduces. This increases band gap and absorption band shifts towards shorter wavelength.<sup>19</sup> The UV absorption band of pure Gd<sub>2</sub>O<sub>3</sub> nanoparticles is around 278nm, whereas TiO<sub>2</sub> is at 344 nm. Gd<sup>+3</sup> doesn't enter into the crystal lattice of TiO<sub>2</sub> but deposits on the surface of TiO<sub>2</sub> matrix. Hence, absorption takes place in shorter wavelength.<sup>21</sup>

The FT-IR spectra of pure TiO<sub>2</sub> and Gd doped TiO<sub>2</sub> are shown in **Fig.5**. The pure TiO<sub>2</sub> shows strong and broad absorption band around 650 cm<sup>-1</sup> corresponds to Ti–O–Ti stretching. Whereas, broad peak found at 3400 cm<sup>-1</sup> is ascribed to OH stretching frequency of water molecule associated with TiO<sub>2</sub> matrix. Further, a medium absorption band at 1650 cm<sup>-1</sup> is observed due to bending vibration of Ti–O. While, Gd doped TiO<sub>2</sub> shows strong and broad Gd–O stretching frequency at 600cm<sup>-1</sup>. But there is increase in intensity of absorption band which is due to presence of Gd<sup>+3</sup> ions along with TiO<sub>2</sub>. Since, stretching frequency of Gd–O and Ti–O–Ti more or less falls in same range with slight disparity. Consequently, the intensity of broad band ranging between 650 cm<sup>-1</sup> to 550 cm<sup>-1</sup> is more in case of Gd doped TiO<sub>2</sub> compared to pure TiO<sub>2</sub>.<sup>17</sup>



### 3.2 Effect of Concentration of Dye on Photodegradation

To study the effect of variation of dye concentration on photocatalysis, the concentration of dye was varied from  $3 \times 10^{-6} \text{ mol dm}^{-3}$  to  $20 \times 10^{-6} \text{ mol dm}^{-3}$  and remaining parameters such as pH and dosage of catalyst were maintained constant. The **Table 1** and **Fig. 6** represents effect of dye concentration on photodegradation. We observed, decrease in rate constant ( $k_{\text{obs}}$ ) with increase in concentration of dye. This can be explained on fact that, initially as the concentration is low, adequate number of dye molecules acquire active sites on surface of  $\text{TiO}_2$  and electrons of photocatalyst get excited from valence band to conduction band creating holes. These holes will react with water molecules, which results in generation of hydroxyl ( $\cdot\text{OH}$ ) free radicals, which are responsible for degradation of dye molecules that are adsorbed on surface of photocatalyst and also the molecules which are near to surface of catalyst<sup>22</sup>. But, when the concentration of dye increases, more number of dye molecules absorb UV light due to which screening effect for photocatalyst occurs. Consequently, photocatalyst may not receive desired intensity of UV light required for the excitation. Hence, the rate of generation of  $\cdot\text{OH}$  free radical decreases and accordingly the rate of degradation decreases.<sup>23</sup>

### 3.3 Effect of Catalyst on Photodegradation.

In view to understand the effect of dosage of catalyst, the photodegradation was carried out by varying catalyst from  $0.1 \text{ g dm}^{-3}$  to  $1 \text{ g dm}^{-3}$  and other parameters such as concentration and pH were maintained as  $3 \times 10^{-6} \text{ dm}^{-3}$  and 7 respectively. The **Table. 1** and **Fig. 7** represents effect of dosage of photocatalyst on photodegradation. The rate constant ( $k_{\text{obs}}$ ) increased as the dosage of photo catalyzed was increased from  $0.1 \text{ g dm}^{-3}$  to  $0.3 \text{ g dm}^{-3}$ , but there after the rate constant started decreasing from  $0.4 \text{ g dm}^{-3}$  to  $1 \text{ g dm}^{-3}$  and the rate of photodegradation was very low at dosage of  $1 \text{ g dm}^{-3}$ .

This observation indicates that, the photocatalytic activity is maximum at certain optimized condition that is  $0.3 \text{ g dm}^{-3}$ . As the dosage of photocatalyst increases, dye molecules get more active sites for adsorption due to increase in surface area of photocatalyst<sup>15</sup>. However, as the dosage exceeds certain limiting value, the degradation decreases because turbidity in solution doesn't allow enough light to reach the catalyst which is essential for excitation. Therefore, there is decreasing trend in rate of degradation.<sup>22</sup>

### 3.4 Effect of pH on Photodegradation.

The pH of solution plays very crucial role in governing the photocatalytic activity of any heterogeneous catalyst<sup>24</sup>. The pH of solution affects the adsorption of dye molecules by altering the surface-charge properties of  $\text{TiO}_2$ . The surface charge of  $\text{TiO}_2$  mainly depends on pH of solution.  $\text{TiO}_2$  has point of zero charge at 6.8 pH,<sup>25</sup> when the pH of solution falls below 6.8 or in acidic solution, the surface of  $\text{TiO}_2$  acquires positive charge and it attracts anions. On other hand,<sup>6</sup> when pH increases more than 6.8 or in alkaline solution, the surface of  $\text{TiO}_2$  acquires negative charge and it attracts cations

To study the effect of pH on rate of photocatalytic degradation, the pH of solution was varied from 4 to 10 and remaining parameters were maintained constant. The **Table. 1** and **Fig.8** represents effect of pH on photodegradation. The rate of degradation increased with increase in pH of solution. The rate of degradation was low at pH 4 and high at pH 10. Such trend may be due to more electrostatic force of attraction between cationic dye molecules and  $\text{TiOH}_2^+$  which is an active species in alkaline condition.<sup>26</sup> But in acidic condition, surface of photocatalyst acquires positive charge and hence the electrostatic repulsion between  $\text{TiO}^-$  and cationic dye molecules doesn't favor adsorption on surface of photocatalyst.<sup>27</sup> Hence the rate of photodegradation decreases. Further, in alkaline condition the rate of formation of hydroxyl radicals is more which favors photodegradation.

### 3.5 Mechanism of Photodegradation & Assessment of Photocatalytic efficiency.

The photodegradation of acriflavine was studied in various conditions viz., UV, UV/ $\text{TiO}_2$ , UV/0.2% Gd- $\text{TiO}_2$ , UV/ 0.3% Gd- $\text{TiO}_2$ , 0.5% Gd- $\text{TiO}_2$ , UV/1.0 % Gd- $\text{TiO}_2$  and other parameters were kept constant,  $[\text{AFN}] = 3 \times 10^{-6}$ ,  $[\text{Photocatalyst}] = 0.3 \text{ g dm}^{-3}$  and  $\text{pH} = 7$ . Variation of  $[\text{AFN}]$ , dosage of Photocatalyst and pH on rate constant values are tabulated in **Table. 1**.

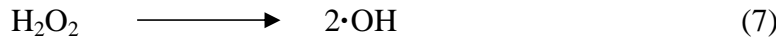
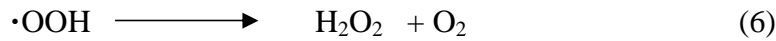
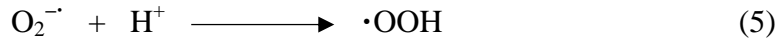
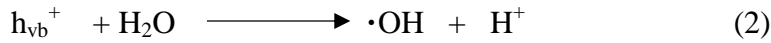
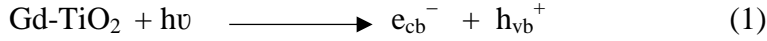
The photo degradation efficiency for various percentage of dopant in  $\text{TiO}_2$  is shown in **Fig. 9a**. The degradation of acriflavine using only UV light can be neglected, because only 13% degradation was achieved in 120 min. The percentage of dopant showed substantial effect on photocatalytic activity of  $\text{TiO}_2$ . The degradation efficiency increased with increase in percentage of dopant up to 0.5% that is 92%, whereas for 1.0% Gd- $\text{TiO}_2$ , the degradation efficiency was reduced to 63%. Such behavior might be due change in surface area to volume ratio of nanoparticles. As dopant concentration increases, the particle size increase, due to which the surface area decreases and hence degradation efficiency decreases<sup>19</sup>. Moreover,  $\text{Gd}^{+3}$  doesn't enter into  $\text{TiO}_2$  matrix rather it deposits on the surface. The increase in concentration of dopant above the optimum value might cover the surface of  $\text{TiO}_2$  due to which  $\text{TiO}_2$  matrix will not receive adequate amount UV light required for excitation. The excess of Gd dopant reduces the photocatalytic capacity of  $\text{TiO}_2$ , possible due to excess of vacancy generated which act as recombination center instead electron scavenger<sup>19</sup>.

The maximum degradation efficiency of 92 % was by 0.5% Gd- $\text{TiO}_2$  compared to bare  $\text{TiO}_2$  which showed only 54% in 120 mins. Among different Gd- $\text{TiO}_2$ , the decreasing order of degradation efficiency was found to be 0.5% Gd- $\text{TiO}_2$ , 92% > 0.3% Gd- $\text{TiO}_2$ , 84% > 0.2% Gd- $\text{TiO}_2$ , 76% > 1.0 % Gd- $\text{TiO}_2$ , 63% >  $\text{TiO}_2$ , 54% > UV, 13%. Since, 0.5% Gd- $\text{TiO}_2$  showed maximum efficiency, further all studies were carried out using 0.5% Gd- $\text{TiO}_2$ . Hence it was observed that, photocatalytic activity of  $\text{TiO}_2$  can be enhanced only by using optimum concentration of Gd. The degradation of acriflavine by 0.5% Gd doped  $\text{TiO}_2$  is shown in **Fig. 9b**.

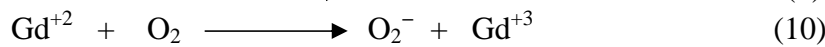
When Ultra-Violet light falls on the surface of photocatalyst, photons having energy equal to or greater than the band gap of semiconductor are absorbed by the electrons. These electrons are excited to conduction band and equal number of holes are created in valence band as shown in eqn (1). Holes ( $h_{\text{vb}}^+$ ) generated in valence band react with water molecules on the surface of photocatalyst which results in formation of hydroxyl free radicals ( $\cdot\text{OH}$ ) as given in eqn (2). These hydroxyl free radicals degrade dye molecules which are adsorbed on



the surface and vicinity of photocatalyst.<sup>28</sup> On other hand, the electrons ( $e_{cb}^-$ ) in conduction band react with dissolved oxygen to produce superoxide ions<sup>20</sup> which helps in avoiding electron-hole recombination as shown in eq(4). Superoxide ion ( $O_2^-$ ) reacts with  $H^+$  ions to form hydroperoxy radical ( $\cdot OOH$ ), which turns into hydrogen peroxide and dissociates in subsequent step to form hydroxyl free radicals ( $\cdot OH$ ). These hydroxyl free radicals take part in dye degradation.<sup>6</sup>



There was enhancement in photocatalytic activity on doping with Gadolinium. The enhanced photocatalytic activity perhaps due to decrease in particle size and increase in surface area.<sup>11</sup> Since, Gadolinium belongs to inner transitional elements which are known to form complex with various organic compounds.<sup>6</sup> The organic compounds generally Lewis bases, such as amines, aldehydes, alcohols, acids, and thiols interact with the half-filled f-orbitals of Gadolinium ions through their functional groups and molecules of substrate concentrate on the surface of Gd-TiO<sub>2</sub> matrix. Higher the accumulation of substrate molecules on the surface of photocatalyst, higher would be the photocatalytic degradation. Such consequences lead to enhancement in the photocatalytic activity.<sup>11</sup> Further, Gadolinium ions have half-filled f-orbitals due to which it can prevent potential recombination of electron-hole pairs by acting as scavenger for electrons of conduction band.  $Gd^{+3}$  ions are stable due to half-filled orbitals, but stability get destroyed when  $Gd^{+3}$  ion traps electron from conduction band to form  $Gd^{+2}$  [eq (9)]. The  $Gd^{+2}$  ion try to return to stable  $Gd^{+3}$  state by transferring an electron to oxygen molecule, it leads to formation of superoxide ion eq (10) which contributes towards photodegradation<sup>29</sup>.



On other hand,  $Gd^{+3}$  ions also act as scavenger for holes through indirect pathway.<sup>29</sup> When TiO<sub>2</sub> is doped with Gadolinium ions, there is a charge imbalance which is compensated by adsorbing more number of  $OH^-$  ions eq(11) on the surface of photocatalyst. The holes generated during photoexcitation react with adsorbed  $OH^-$  ions which lead to formation of hydroxyl radicals<sup>30</sup> [eq(12)].



This conclusion can also be fortified due to high photocatalytic degradation which is observed at pH 10.

#### 4. Conclusion.

Eco friendly hydrothermal route was used for the synthesis of TiO<sub>2</sub> and Gd doped TiO<sub>2</sub> nanoparticles. It was confirmed by various characterization techniques. Acriflavin was degraded under UV light using TiO<sub>2</sub> and Gd doped TiO<sub>2</sub> nanoparticles. Among various percentage of Gd doped TiO<sub>2</sub>, the maximum efficiency was found for 0.5% Gd doped TiO<sub>2</sub>. The degradation efficiency increases only up to optimum percentage of dopant. The photocatalytic activity of TiO<sub>2</sub> was enhanced by Gd due to its complex forming ability with dye molecules. Gd is found to be reliable dopant to enhance the photocatalytic activity of TiO<sub>2</sub>. We have also further analyzed the effect of various parameters on the photocatalytic dye degradations. Following results were obtained.

- The maximum photocatalytic activity was observed for the dye concentration, [AFN] =  $3 \times 10^{-6}$  mol dm<sup>-3</sup>
- The photocatalytic activity was observed maximum at certain optimized catalyst dosage of 0.3g dm<sup>-3</sup>
- The photo-catalytic activity goes on increasing as pH value was increased, the maximum was observed at pH 10.

#### References:

1. Hosseini SA, Moalemzade P. CuFe<sub>2-x</sub> Lu<sub>x</sub>O<sub>4</sub> nanoparticles : synthesis through a green approach and its photocatalyst application. *J Mater Sci Mater Electron*. 2016;37(8):8802-8806. doi:10.1007/s10854-016-4905-7
2. Webb SF. A Data Based Perspective on the Environmental Risk Assessment of Human Pharmaceuticals 11 - Aquatic Risk Characterisation. In: Kümmerer K, ed. *Pharmaceuticals in the Environment*. Springer, Berlin, Heidelberg; 2001:202-219. doi:10.1007/978-3-662-04634-0\_16
3. Kulkarni RM, Malladi RS, Hanagadakar MS, Doddamani MR, Santhakumari B, Kulkarni SD. Ru-TiO<sub>2</sub> semiconducting nanoparticles for the photo-catalytic degradation of bromothymol blue. *J Mater Sci Mater Electron*. 2016;27(12):13065-13074. doi:10.1007/s10854-016-5449-6
4. Gupta V., Kraft S., Samuelson J. Purification and properties related compounds. *J Chromatogr A*. 1967;26:158-163. doi:10.1016/S0021-9673(01)98850-8
5. CDH fine C. Acriflavin Hydrochloride CAS No 8063-24-9 MATERIAL SAFETY DATA SHEET SDS / MSDS.
6. Ajmal A, Majeed I, Malik RN, Idriss H, Nadeem MA. Principles and mechanisms of photocatalytic dye degradation on TiO<sub>2</sub> based photocatalysts: A comparative overview. *RSC Adv*. 2014;4(70):37003-37026. doi:10.1039/c4ra06658h
7. Choudhury B, Borah B, Choudhury A. Extending Photocatalytic Activity of TiO<sub>2</sub> Nanoparticles to Visible Region of Illumination by Doping of Cerium. *Photochem Photobiol*. 2012;88(2):257-264. doi:10.1111/j.1751-1097.2011.01064.x

8. Choudhury B, Borah B, Choudhury A. Ce – Nd codoping effect on the structural and optical properties of TiO<sub>2</sub> nanoparticles. *Mater Sci Eng B*. 2013;178(4):239-247. doi:10.1016/j.mseb.2012.11.017
9. Sci C, Weber AS, Grady AM, Koodali RT, Weber AS, Grady AM. Catalysis Science & Technology Lanthanide modified semiconductor photocatalysts. *Catal Sci Technol*. 2012;683-693. doi:10.1039/c2cy00552b
10. Zhou Y, Luo Q, Liu Y, Li D, Yang L, Cao F. Solvothermal synthesis of hollow flower-like Gd-doped - with enhanced photocatalytic performance. *J Mater Sci Mater Electron*. 2018;29(01):446-454. doi:10.1007/s10854-017-7933-z
11. Adyani SM, Ghorbani M. A comparative study of physicochemical and photocatalytic properties of visible light responsive Fe, Gd and P single and tri-doped TiO<sub>2</sub>. *J Rare Earths*. 2018;36(1):72-85. doi:10.1016/j.jre.2017.06.012
12. Al-hamdi AM, Sillanpää M, Dutta J. Gadolinium doped tin dioxide nanoparticles : an efficient visible light active photocatalyst. *J Rare Earths*. 2015;33(12):1275-1283. doi:10.1016/S1002-0721(14)60557-3
13. Paul S, Chetri P, Choudhury B, Ahmed GA, Choudhury A. Enhanced visible light photocatalytic activity of Gadolinium doped nanocrystalline titania : An experimental and theoretical study. *J Colloid Interface Sci*. 2015;439:54-61. doi:10.1016/j.jcis.2014.09.083
14. Hunagund SM, Desai VR, Kadadevarmath JS, Barretto DA, Vootla S, Sidarai AH. Biogenic and chemogenic synthesis of TiO<sub>2</sub> NPs: Via hydrothermal route and their antibacterial activities. *RSC Adv*. 2016;6(99):97438-97444. doi:10.1039/C6RA22163G
15. Kulkarni RM, Malladi RS, Hanagadakar MS, Doddamani MR, Bhat UK. Ag-TiO<sub>2</sub> nanoparticles for photocatalytic degradation of lomefloxacin. *Desalin Water Treat*. 2016;57(34):16111-16118. doi:10.1080/19443994.2015.1076352
16. Lee HY, Kale GM. Hydrothermal Synthesis and Characterization of Nano-TiO<sub>2</sub>. *Int J Appl Ceram Technol*. 2008;5(6):657-665. doi:10.1111/j.1744-7402.2008.02248.x
17. Hunagund SM, Desai VR, Barretto DA, et al. Journal of Photochemistry and Photobiology A : Chemistry Photocatalysis effect of a novel green synthesis gadolinium doped titanium dioxide nanoparticles on their biological activities. *Journal Photochem Photobiol A Chem*. 2017;346:159-167. doi:10.1016/j.jphotochem.2017.06.003
18. Di Wu, Chen Li, Dashuai Zhanga, b, LiLi Wang, Xiaopeng Zhang ZS, Lina Q. Enhanced photocatalytic activity of Gd<sup>3+</sup> doped TiO<sub>2</sub> and Gd<sub>2</sub>O<sub>3</sub> modified TiO<sub>2</sub> prepared via ball milling method. *J Rare Earths*. 2019;37(8):845-852. doi:https://doi.org/10.1016/j.jre.2018.10.011
19. Mahalakshmi M, Arabindoo B, Palanichamy M, Murugesan V. Preparation, Characterization, and Photocatalytic Activity of Gd<sup>3+</sup> Doped TiO<sub>2</sub> Nanoparticles. *J Nanosci Nanotechnol*. 2007;7(9):3277-3285. doi:10.1166/jnn.2007.689
20. Paul S, Choudhury B, Choudhury A. Magnetic property study of Gd doped TiO<sub>2</sub> nanoparticles. *J Alloys Compd*. 2014;601:201-206. doi:10.1016/j.jallcom.2014.02.070
21. Anishur Rahman ATM, Vasilev K, Majewski P. Ultra small Gd<sub>2</sub>O<sub>3</sub> nanoparticles: Absorption and emission properties. *J Colloid Interface Sci*. 2011;354(2):592-596.

- doi:10.1016/j.jcis.2010.11.012
22. Barka N, Qourzal S, Assabbane A, Nounah A, Ait-Ichou Y. Photocatalytic degradation of an azo reactive dye, Reactive Yellow 84, in water using an industrial titanium dioxide coated media. *Arab J Chem.* 2010;3(4):279-283. doi:10.1016/j.arabjc.2010.06.016
  23. Haque MM, Muneer M. TiO<sub>2</sub>-mediated photocatalytic degradation of a textile dye derivative, bromothymol blue, in aqueous suspensions. *Dye Pigment.* 2007;75(2):443-448. doi:10.1016/j.dyepig.2006.06.043
  24. Alaton I, Balcioglu IA, Bahnemann D. Advanced oxidation of a reactive dyebath effluent: comparison of O<sub>3</sub>, H<sub>2</sub>O<sub>2</sub>/UV-C and TiO<sub>2</sub>/UV-A processes. *Water Res.* 2002;36(March):1143-1154.
  25. Gimeno O, Rivas J, Encinas A, Beltran F. Application of Advanced Oxidation Processes to Mefenamic Acid Elimination. *Int J Nucl Quantum Eng.* 2010;4(6):1104-1106.
  26. Muruganandham M, Swaminathan M. Solar photocatalytic degradation of a reactive azo dye in TiO<sub>2</sub>-suspension. *Sol Energy Mater Sol Cells.* 2004;81(4):439-457. doi:10.1016/j.solmat.2003.11.022
  27. Qamar M, Saquib M, Muneer M. Photocatalytic degradation of two selected dye derivatives, chromotrope 2B and amido black 10B, in aqueous suspensions of titanium dioxide. *Dye Pigment.* 2005;65(1):1-9. doi:10.1016/j.dyepig.2004.06.006
  28. Barakat MA, Kumar R. *Photocatalytic Activity Enhancement of Titanium Dioxide Nanoparticles.* 1st ed. Springer International Publishing; 2016. doi:10.1007/978-3-319-24271-2
  29. Xu AW, Gao Y, Liu HQ. The preparation, characterization, and their photocatalytic activities of rare-earth-doped TiO<sub>2</sub> nanoparticles. *J Catal.* 2002;207(2):151-157. doi:10.1006/jcat.2002.3539
  30. Karimi L, Zohoori S, Yazdanshenas ME. Photocatalytic degradation of azo dyes in aqueous solutions under UV irradiation using nano-strontium titanate as the nanophotocatalyst. *J Saudi Chem Soc.* 2014;18(5):581-588. doi:10.1016/j.jscs.2011.11.010

**Table 1.** Effect of variation of [AFN], Dosage of Photo-catalyst and pH on rate constant

[AFN]	Dosage of Photo-catalyst g dm <sup>-3</sup>	pH	Rate constant k <sub>obs</sub> s <sup>-1</sup>
3 x 10 <sup>-6</sup>	0.3	7	0.74 x10 <sup>-2</sup>
5 x 10 <sup>-6</sup>	0.3	7	0.44 x10 <sup>-2</sup>
7 x 10 <sup>-6</sup>	0.3	7	0.42 x10 <sup>-2</sup>
10 x 10 <sup>-6</sup>	0.3	7	0.33 x10 <sup>-2</sup>
3 x 10 <sup>-6</sup>	0.1	7	0.42 x10 <sup>-2</sup>
3 x 10 <sup>-6</sup>	0.2	7	0.69 x10 <sup>-2</sup>
3 x 10 <sup>-6</sup>	0.3	7	0.47 x10 <sup>-2</sup>
3 x 10 <sup>-6</sup>	0.4	7	0.29 x10 <sup>-2</sup>
3 x 10 <sup>-6</sup>	0.5	7	0.43 x10 <sup>-2</sup>
3 x 10 <sup>-6</sup>	1.0	7	0.66 x10 <sup>-2</sup>
3 x 10 <sup>-6</sup>	0.3	4	0.60 x10 <sup>-2</sup>
3 x 10 <sup>-6</sup>	0.3	5	0.66 x10 <sup>-2</sup>
3 x 10 <sup>-6</sup>	0.3	7	0.74 x10 <sup>-2</sup>
3 x 10 <sup>-6</sup>	0.3	9	1.23 x10 <sup>-2</sup>
3 x 10 <sup>-6</sup>	0.3	10	1.44 x10 <sup>-2</sup>

## List of Figures

**Fig.1a** XRD pattern for pure TiO<sub>2</sub>

**Fig.1b** XRD pattern for pure Gd doped TiO<sub>2</sub>

**Fig.2** The FESEM images (a) (b) pure TiO<sub>2</sub> and (c), (d) Gd doped TiO<sub>2</sub>.

**Fig. 3** UV-visible spectra pure TiO<sub>2</sub> &Gd doped TiO<sub>2</sub>.

**Fig.4** Tauc's plot.

**Fig. 5** FT-IR Spectra of pure TiO<sub>2</sub> and Gd-TiO<sub>2</sub>

**Fig. 6** Effect of variation of dye concentration on rate of Photo-degradation.

**Fig.7** Effect of photo-catalyst dosage on rate of Photo-degradation.

**Fig. 8** Effect of pH on rate of photo-degradation.

**Fig. 9a** % Degradation efficiency by various treatment methods with respect to time.

**Fig.9b** Degradation of AFN by 0.5%Gd-TiO<sub>2</sub> with time.

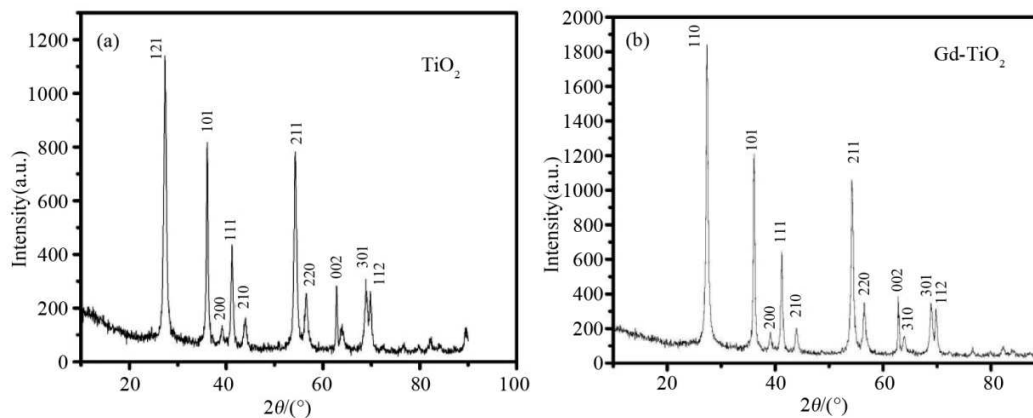


**Fig.1** XRD pattern for pure TiO<sub>2</sub> (a) and Gd doped TiO<sub>2</sub> (b).



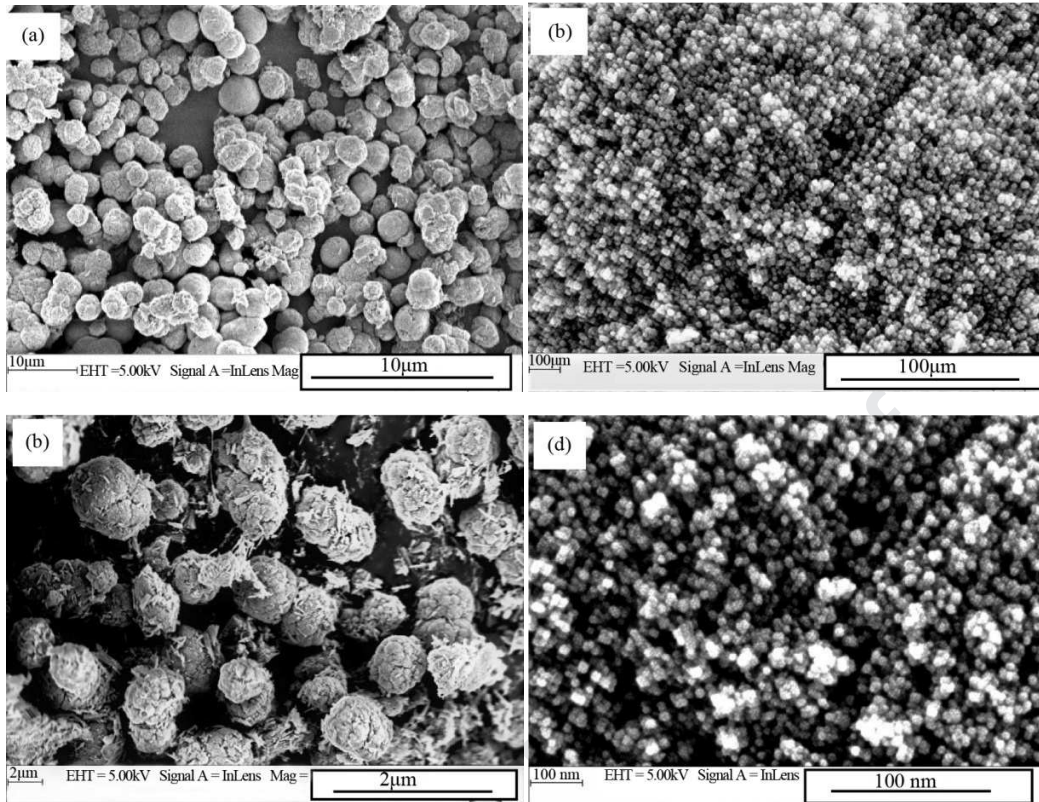


**Fig.2** FESEM images pure  $\text{TiO}_2$  10  $\mu\text{m}$  (a) and 100 nm (b) and Gd doped  $\text{TiO}_2$  2  $\mu\text{m}$  (c) and 100 nm (d).

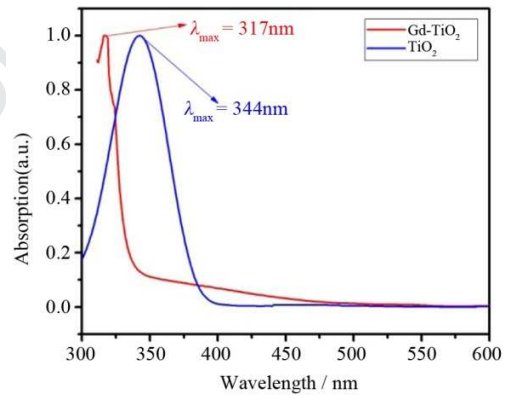


**Fig. 3** UV-visible spectra pure  $\text{TiO}_2$  & Gd doped  $\text{TiO}_2$ .

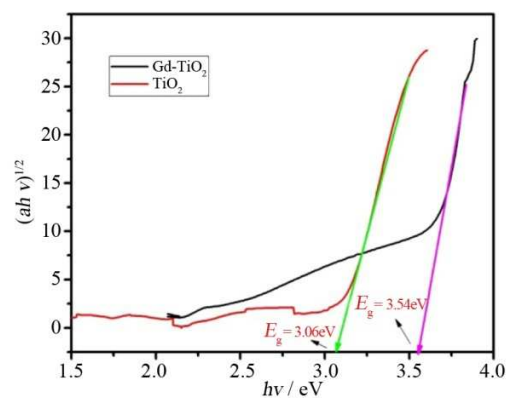


Fig.4 Tauc's plot.

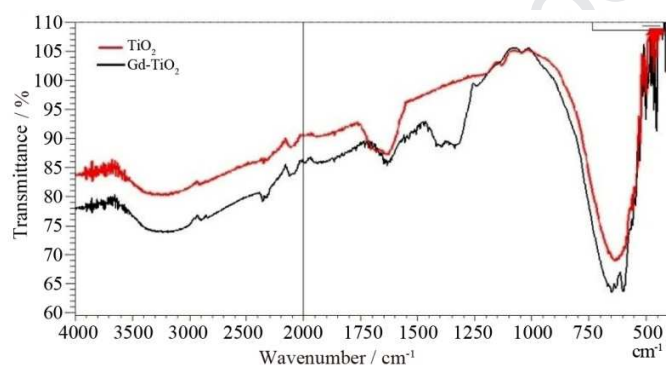
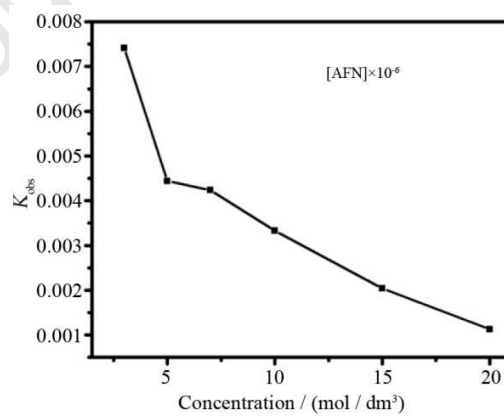
Fig. 5 FT-IR Spectra of pure TiO<sub>2</sub> and Gd-TiO<sub>2</sub>.

Fig. 6 Effect of variation of dye concentration on rate of Photo-degradation.

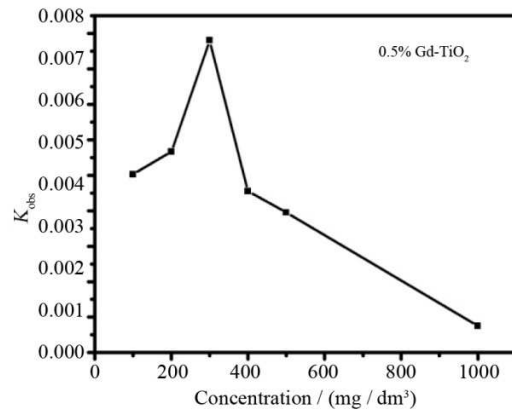


Fig.7 Effect of photo-catalyst dosage on rate of Photo-degradation.

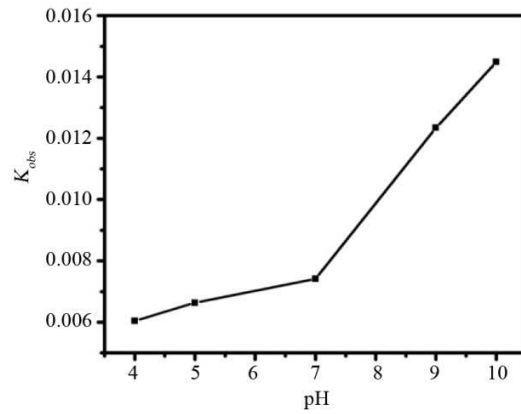


Fig. 8 Effect of pH on rate of photo-degradation.

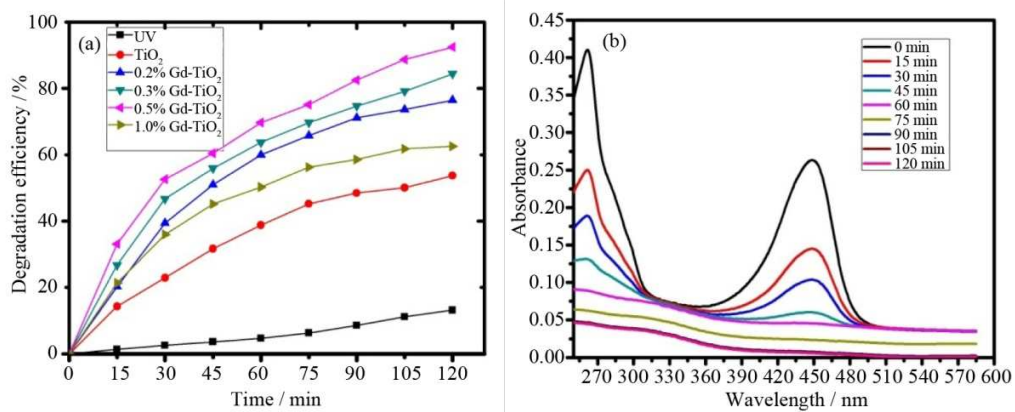


Fig. 9 % Degradation efficiency by various treatment methods with respect to time (a) and degradation of AFN by 0.5% Gd-TiO<sub>2</sub> with time (b).

## Graphical Abstract

Photocatalytic Mechanism of Gd doped  $\text{TiO}_2$ :  $\text{Gd}^{3+}$  ions enhance the photocatalytic activity by avoiding potential recombination of electrons and holes through different pathways.

